The 2016 World Congress on
Advances in Civil, Environmental, and Materials Research (ACEM16)
Jeju Island, Korea, August 28-September 1, 2016

Wind Tunnel Study on Wind Flow upwind and downwind of the Full-scale Wind Barrier and its Aerodynamic Wind Loads

*Yang Su[1)], Yongle Li[2)], Chen Fang[3)], Lei Wang[4)] and Xinli Meng[5)]

[1)] *Department of Bridge Engineering, Southwest Jiaotong University, Chengdu, Sichuan 610031, China*
[2)] *ShangFeng Science and Technology Co., LTD, Taiyuan, Shanxi 030000, China*
[1)] *pkingdream@126.com*
[2)] *lele@swjtu.edu.cn*
[3)] *1454457971@qq.com*
[4)] *wangleiyuhua@163.com*
[5)] *1185790187@qq.com*

(Received keep as blank , Revised keep as blank , Accepted keep as blank)

Abstract. The present study provided a deeper understanding of wind flow upwind and downwind of the wind barriers with porosities of 36.5% and height of 3.5m and its aerodynamic wind loads by means of a full-scaled wind tunnel simulation. Velocities were measured using cobra probes and the mean velocity field and turbulence intensity were obtained and discussed. Aerodynamic drag forces of wind barrier blades were measured using a balance (5Kg) and its distribution law was analyzed. The results show that the pore size of the barrier blade and different forms of the barrier have a slight influence on mean streamwise velocities and turbulence intensity upwind of the barrier. However, some influences on mean streamwise velocities and turbulence intensity are found downwind of the barrier. From left to right, drag coefficients of barrier blades at three cases increase at first and then decrease.

Keywords: wind barrier blade; full-scale; wind tunnel test; wind flow; wind load;

1. Introduction

In recent years, with the rapid development of railway and the raising speed of train, the running safety of train becomes more and more important. As one of the important and effective means, wind barriers are used to reduce wind-induced accidents of trains, so study on wind barriers becomes a hot research topic increasingly. Three main research methods are applied to study wind barriers: field experiment, wind tunnel test and numerical simulation, respectively.

Porous barriers were used to investigate the characteristics of streamwise turbulence spectra by means of field experiment. It was observed that the frequencies of the generated turbulence are related to the velocity gradients in the region where generation occurs (Richardsona 1995). Aiming at the sound barrier, a field experiment was carried out with respect to three important factors: vehicle type, vehicle speed and the vehicle-barrier

---

[1), 3), 4), 5)] Ph.D
[2)] Professor

separation distance (Wang and Wang et al. 2013). However, the research on mechanism for wind barriers is very difficult to carry out by means of the field experiment, due to satisfying different kinds of harsh conditions, such as security, difficulty et al. So the data of field experiment about wind barriers for traffic is limited.

Scale section model wind tunnel test is another effective way to explore the protection effect of wind barriers. Various technical textiles with different opening sizes, opening size distributions, open areas and flow reduction coefficients were tested by a scale barrier model wind tunnel test to compare their efficiency in reducing wind speed (Dierickx and Gabriels et al. 2001). Experiments in the wind tunnel were carried out to compare the effects on wind velocity reduction of vertical and inclined screens and the result showed that screens inclined against the wind were more effective than screens inclined with the wind (Dierickx and Cornelis et al. 2003). Previous study provided a deeper understanding of mean flow regime behind fences with different porosities at different wind velocities by means of a scaled wind tunnel simulation. The result showed that the optimal porosity was found to be around 0.2 or 0.3 (Dong and Luo et al. 2007). Wu and Zou et al. 2013 compared shelter quality of wind barriers of different porosity, row space and row number based on wind-tunnel measurements and suggested the optimal porosity of 0.3~0.4 for wind barriers. Research objects in previous studies mainly are scale models of barriers. It is difficult to definite the scale effect and errors will be found under the condition of the holes of barriers being very small. Moreover, the study on effects of local details such as pore size and holes shape is difficult to obtain.

As for the numerical simulation, RANS (Reynolds-averaged Navier-Stokes equations) simulations using three variants ofκ-εturbulence closure models had been performed to analyze wind flow characteristics behind an isolated fence located on a flat surface without roughness elements. A value of 0.35 was found as the optimum value among the studied porosities (Santiago and Martín et al. 2007). Using CFD simulations, the effects of fence porosity, fence height, and the distance between the adjacent fences were investigated (Bitog and Lee et al. 2009). The work of (Telenta and Batista et al. 2015) was focused on a parametric numerical study of the barrier's bar inclination shelter effect in crosswind scenario. However, there are some deficiencies: the turbulence and separated flow are difficult to be simulated accurately. So the accuracy of simulation results is relatively limited.

Aiming at the force test, previous studies mainly explored the aerodynamic loads of the whole structure of barriers by a scale model wind tunnel test. Huoyue and Yongle et al. 2015 investigated the aerodynamic loads on barriers under uniform flow and discussed the effect of aerodynamic interactions between vehicles and barriers. For one thing, the impact of scale effect is difficult to definite clearly. The reliability of results obtained by scale model wind tunnel tests is expecting for further research. For another, it is rare to find the research about the aerodynamic loads on barrier blades. So it is necessary to investigate the aerodynamic wind loads by means of a full-scaled wind tunnel simulation.

In conclusion, there are still some problems of the study on wind barriers. Researchers have attempted to investigate wind barriers using the full-scale barrier model wind tunnel test. In our study, three cases of barrier blades are compared with each other to analyze the effects of pore size and different forms of the barrier on the mean streamwise velocity and turbulence intensity upwind and downwind of barriers. Also aerodynamic loads on each of the barrier blade are tested. The results could provide a reference to the design of wind barriers.

2. Full-scaled wind barrier wind tunnel tests

2.1 Full-scaled wind barrier and Test methodology

The experiments were conducted in the XNJD-3 wind tunnel with a top velocity near 16.5 m/s. The turbulence intensity of the free-stream flow I_x is less than 1.5%. It is a closed circuit facility and comprises of a boundary test section that is 36 m long, 22.5 m wide and 4.5 m high.

The test was carried out for three cases of barrier blades (Fig. 1, Fig. 2 and Table 1) which were produced according to the requirements of practical engineering. The porosity, height and length of the whole structure of wind barriers are 36.5%, 3.5m and 4.4m, respectively. All of the cases were carried out in wind environments with uniform flow.

With consideration of influences of flow around the end of the barrier and blockage ratio of the models to the cross-section of the test section on the experiment results, the wind barrier is placed perpendicular to the wind direction and vertically placed in the wind tunnel, in another word, the bottom of the barrier clings to the wall (surface) of the wind tunnel (Fig. 3 and Fig. 4).The illustration of the barrier model and the coordinate system used in the wind tunnel tests is shown in Fig.3. Then we can calculate the blockage ratio of the models (15.6%) by using the height of the barrier (3.5m) to divide the width of the tunnel (22.5m). According to some research, a blockage ratio up to 14% is acceptable in practical engineering (Suzuki and Tanemoto et al. 2003). So blockage ratio meets the requirements basically.

In a force test, the installation convenience, measurement range and measurement accuracy should be taken into consideration, and the interference of cross beam (see Fig.1(b)) on the flow field could not be ignored during the wind field tests. So the framework of the barrier is divided into three sections: 1.7m, 1.7m and1.0m, respectively. According to the experimental contents, there are two arrangement forms of barrier blades: form 1 (see Fig.1(b)) and form 2 (see Fig.14). The form 1 is “1.7m+1.7m+1.0m” from top to bottom, which is used in the wind field tests. The form 2 is “1.7m+1.0m+1.7m”, which is used in the force tests.

Wind velocity measurements in this study were carried out at distances away from the barrier of -1.0H, -0.5H, 0.5H, 1.26H, 2.51H, 3.0H, 4.0H, 5.0H, 6.0H and 8.0H along the longitudinal axis of the test section. It should be pointed out that distances from the barrier of 1.26H (4.4m) and 2.51H (8.8m) are the center of track at windward side and leeward side with reference to a railway bridge in practical engineering, respectively. At each location, wind velocity was measured at sixteen different heights: 0.38m, 0.68m, 0.98m, 1.28m, 1.58m, 1.88m, 2.18m, 2.48m, 3.08m, 3.68m, 4.28m, 4.88m, 5.48m, 6.08m, 6.68m and 7.28m above the surface. To assure that the same initial wind speed was applied to all tests, a reference wind velocity was measured at a distance of -2H and a height of 1.935m windward of the screen (see Fig.4).

Table1 Parameters of wind barrier blades

Case	porosity rates of baldes	Pore size (mm)	Width(mm)	Barrier form
Model-1	36.5%	6	300	Porous
Model-2	36.5%	16	300	Porous
Model-3	0%	0	203	Bar-type

(a) The 1# and 2# barrier blades (b) The porous wind barrier in the wind tunnel

Fig. 1 Barrier blades and arrangement form for the porous barrier

(a) The 3# barrier blade (b) The wind barrier with longitudinal bars in the wind tunnel

Fig. 2 Barrier blades and arrangement form for the bar-type barrier

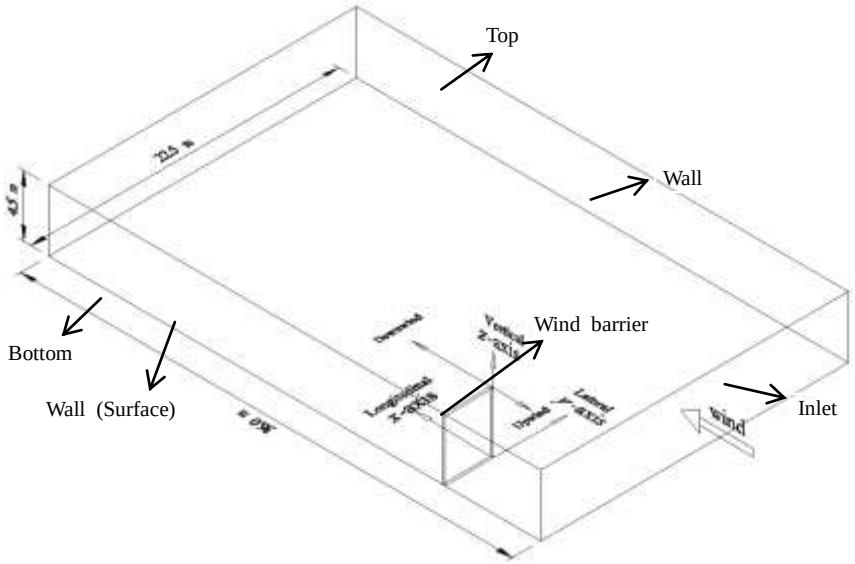

Fig. 3 Illustration of the barrier model and the coordinate system used in the wind tunnel tests.

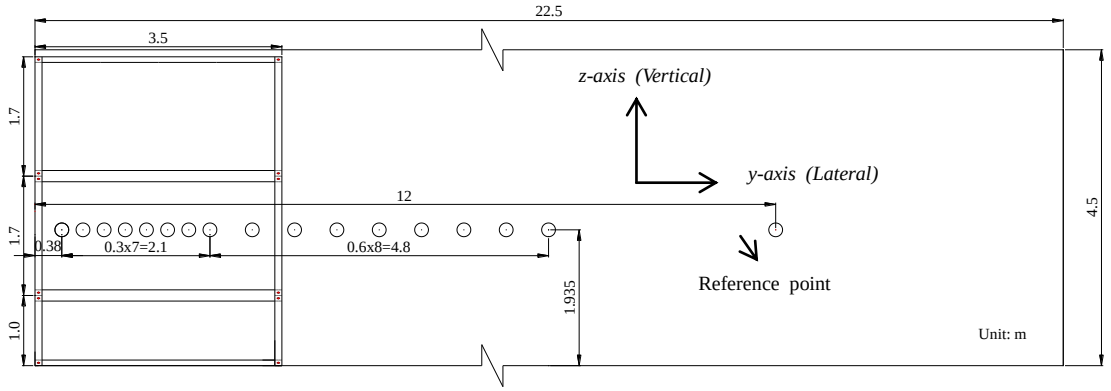

(a) Side view from inlet

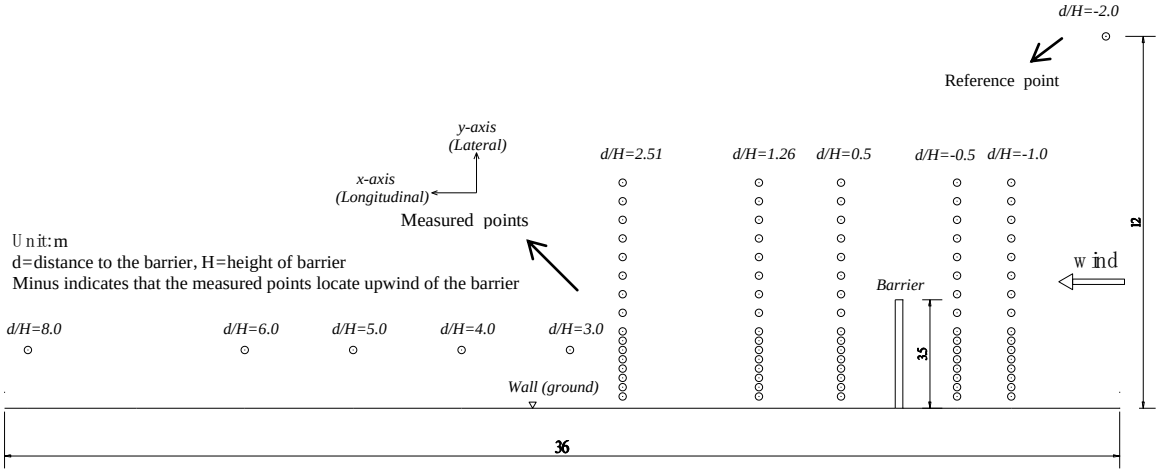

(b) Top view

Fig. 4 Locations of wind velocity measurements in the test section

3. Results and discussion

3.1 Mean velocity field and turbulence intensity

Airflow fields behind barriers are complicated by the presence of both the bleed flow that passes through the gaps in the barriers and the displaced flow that passes over the barriers. However, the airflows over wind barriers could be mainly regarded as two-dimensional. The airflow mainly moves in the lateral (*y*-axis, also being named as the direction along the height of the barrier) and longitudinal (*x*-axis) directions, with little vertical motion along the *z*-axis (see Fig.3). Furthermore, what we concern most is that the characteristics of flow fields in streamwise (horizontal) direction which is the worst wind direction of train accidents. So flow fields in streamwise direction under different cases of barriers are mainly talked about in our study.

The form 1(1.7m+1.7m+1.0m, see Fig.1(b)) is used in the wind field tests. Mean streamwise wind velocities of measured points located at different positions are collected. Variations of the mean streamwise velocity profiles at three cases of barrier blades are shown in Fig.5 and Fig.6 (the streamwise velocity is normalized by the free-stream velocity U_0 (11m/s), and height is normalized by the barrier height *H*). Differences are large for mean streamwise velocity profiles upwind and downwind of the barrier at each case of the barrier blade.

Looking at the results from Fig.5, mean streamwise velocities increase with the increasing of height above the surface upwind of the barrier. An intersection point is found on the mean streamwise velocity profiles at distances of *-1.0H* (*d/H=-1.0*) and-*0.5H* (*d/H=-0.5*) at each case of the barrier blade. Mean streamwise wind velocities at the distance of *-1.0H* away from the barrier are bigger than corresponding velocities at the same height at the distance of *-0.5H* below the intersection point, while it leads to the opposite result above the intersection point. The height of intersection point is almost equal to the height of shear layer of streamwise velocity profiles downwind of the barrier. Mean streamwise wind velocities upwind of the barrier are all less than the free-stream velocity. This phenomenon could be explained as that when the approach flow field flows through barriers, a part of flow will reverse back to the opposite direction because of the resistant of barriers. Then a portion of approaching flow is counteracted by the reverse flow, which causes the loss of wind energy. So it leads to the lower of mean streamwise wind velocities upwind of the barrier.

As for the mean streamwise velocity profiles downwind of the barrier (see Fig.6), an obvious shear layer is found. The height of the shear layer is in the region of $1.0 < y/H < 1.5$. The aero below the height of shear layer is regarded as the influence aero of wind barriers (also being called the wind-resistant region). The aero above the height of shear layer is named as external flow field. For each case of the barrier blade, mean streamwise velocity distribution is non-uniform at the distance of *0.5H* away from the barrier, compared to distances of *d/H=1.26* and *d/H=2.51.* This attributes to that flow field is uneven at the distance of *d/H=0.5* and becomes more stable with the increasing of distances away from the barrier.

Great differences of mean streamwise velocity profiles downwind of the barrier between porous barriers (Model-1 and Model-2) and bar-type barriers (Model-3) are found. This is mainly because that the holes of the porous barrier are relatively uniform while the bar-type barriers being not. Some measured points just locate behind the barrier blades and other points just are situated between the adjacent two barrier blades. So the streamwise velocity profiles downwind of bar-type barriers are relatively uneven.

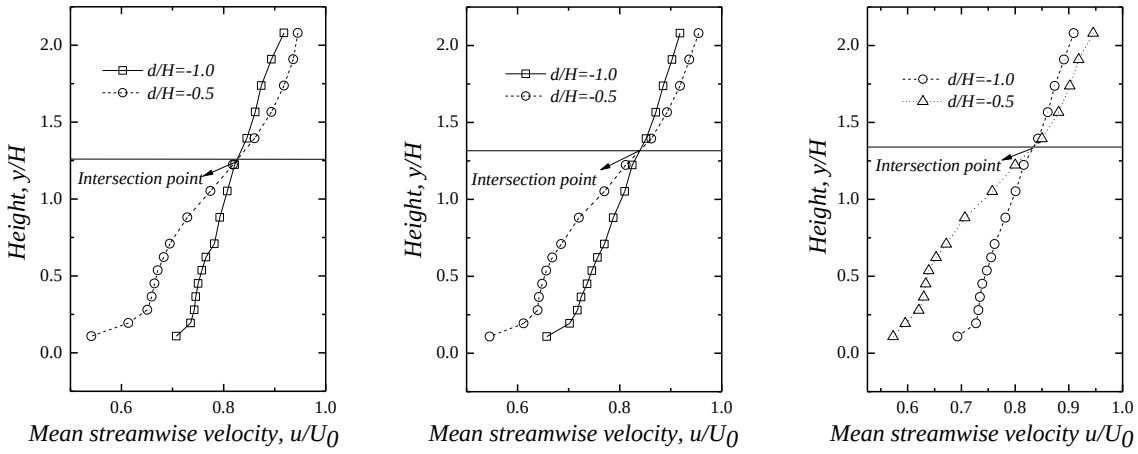

(a) Model-1 (b) Model-2 (c) Model-3

Fig. 5 Variations in the mean streamwise (horizontal) velocity profiles upwind of the wind barrier. *H*=height of the wind barrier, U_0= free-stream velocity (11m/s), *U(y)*= wind velocity at height *y*, *d*=distance to the barrier

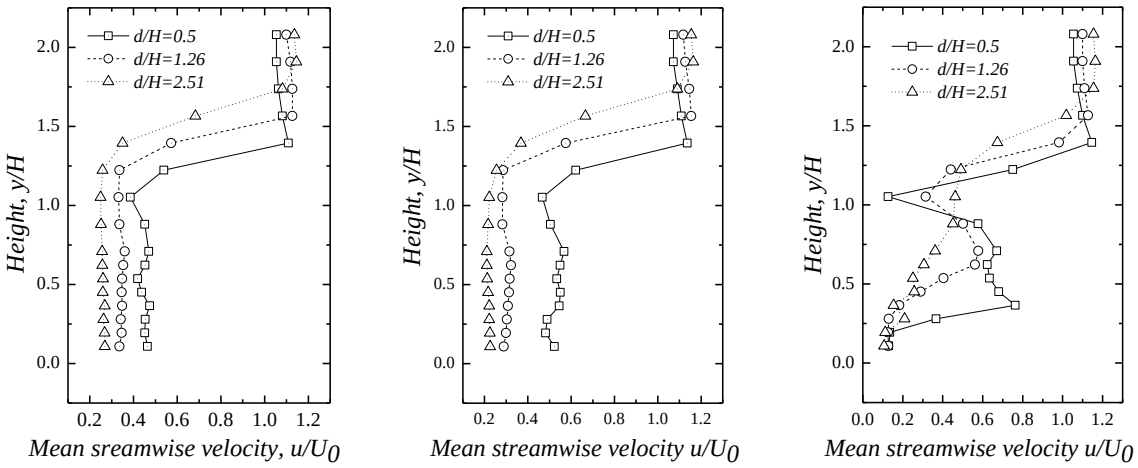

(a) Model-1 (b) Model-2 (c) Model-3

Fig. 6 Variations in the mean streamwise (horizontal) velocity profiles downwind of the wind barrier. *H*=height of the wind barrier, U_0= free-stream velocity (11m/s), *U(y)*= wind velocity at height *y*, *d*=distance to the barrier

3.1.1 Effects of pore size

The following discussion will focus on the effects of pore size of the barrier blade on mean streamwise velocities and turbulence intensity at different distances away from the barrier and heights above the surface. Two cases of Model-1 and Model-2 are compared with each other (Fig.1 and Table1). Pore sizes of Model-1 and Model-2 are 6mm and16mm, respectively.

Fig.7~Fig.11 show the streamwise velocity and turbulence intensity profiles of the flow field as a function of height at different positions. It is shown that the streamwise velocity and turbulence intensity profiles of the flow field are almost similar upwind of the barrier, indicating that the pore size has little effect on the characteristics of flow field upwind of the barrier. Downwind of the barrier, great differences of mean streamwise velocity and turbulence intensity profiles below the height of the shear layer are found at the distance of 0.5H (*d/H=0.5*) away from the barrier, while it shows a same trend above the height of the shear layer. The more distances away from the barrier, the smaller differences of mean streamwise velocity and

turbulence intensity profiles. Looking at the results obtained with the distance of 2.51H *(d/H=2.51)* away from the barrier, mean streamwise velocity and turbulence intensity profiles are in relatively good agreement with each other.

On the whole, there exists some effects of pore size on the mean streamwise velocity and turbulence intensity profiles downwind of the barrier. It shows a decreasing in influence degree of pore size with the increasing of the distance away from the barrier. This is mainly because that the airflow becomes more and more stable with the increasing of the distance away from the barrier. The barrier at the case of Model-1 gives a similar protection with the case of Model-2 from the aspect of mean streamwise velocity. However, the turbulence intensity is relatively uniform at the case of Model-1.

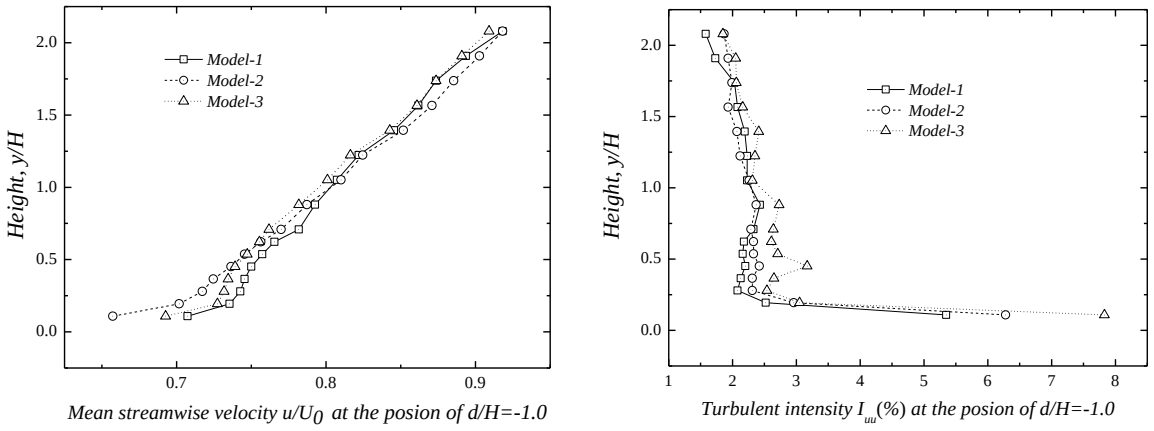

(a) (b)

Fig. 7 Mean streamwise velocity and turbulence intensity profiles of the flow field as a function of height at the position of *d/H=-1.0*. (a) mean velocity profiles and (b) turbulence intensity profiles. *H*=height of the wind barrier, U_0= free-stream wind velocity (11m/s), *U(y)*= wind velocity at height *y*, *d*=distance to the barrier

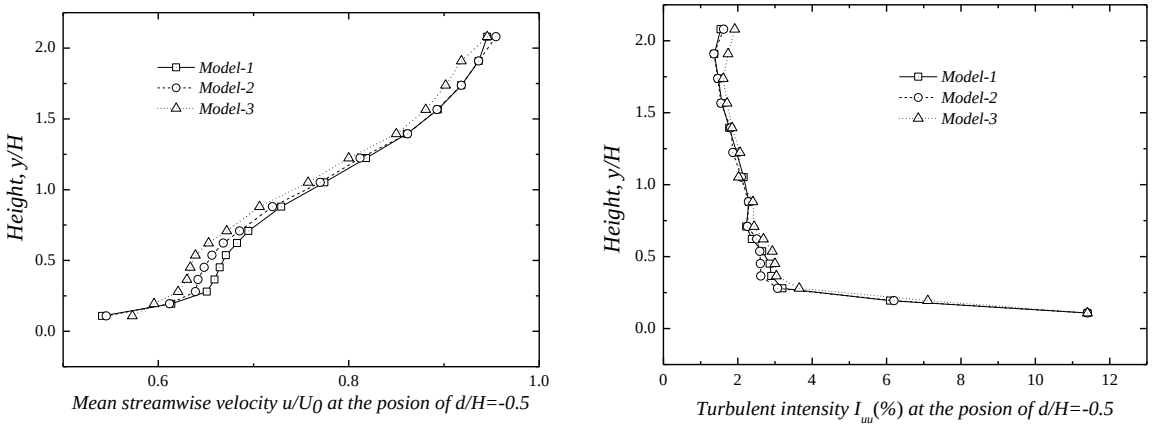

(a) (b)

Fig. 8 Mean streamwise velocity and turbulence intensity profiles of the flow field as a function of height at the position of *d/H=-0.5*. (a) mean velocity profiles and (b) turbulence intensity profiles. *H*=height of the wind barrier, U_0= free-stream wind velocity (11m/s), *U(y)*= wind velocity at height *y*, *d*=distance to the barrier

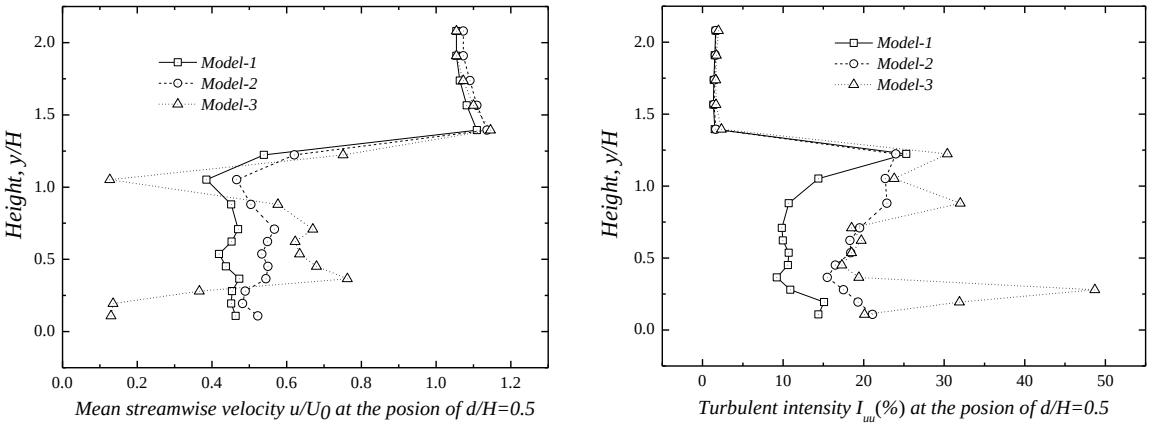

(a) (b)

Fig. 9 Mean streamwise velocity and turbulence intensity profiles of the flow field as a function of height at the position of *d/H=0.5*. (a) mean velocity profiles and (b) turbulence intensity profiles. *H*=height of the wind barrier, U_0= free-stream wind velocity (11m/s), *U(y)*= wind velocity at height *y*, *d*=distance to the barrier

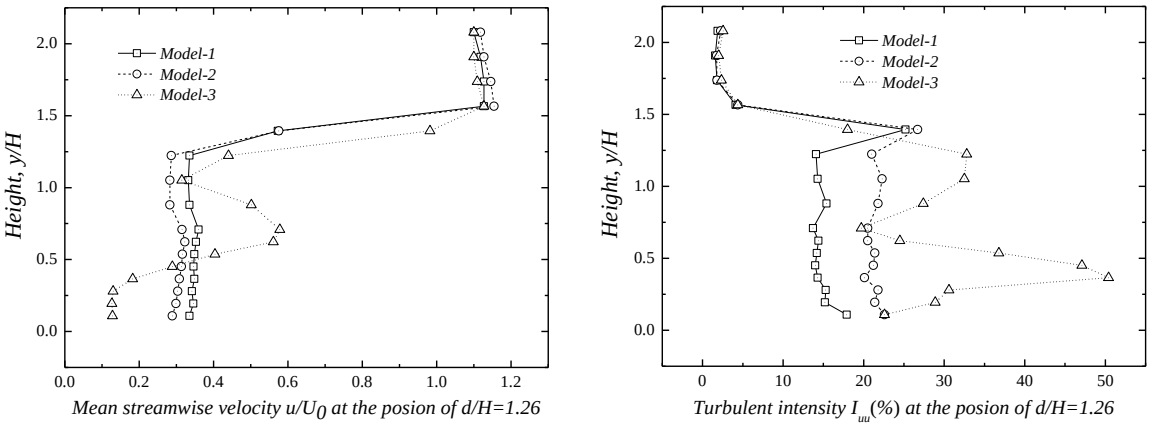

(a) (b)

Fig. 10 Mean streamwise velocity and turbulence intensity profiles of the flow field as a function of height at the position of *d/H=1.26*. (a) mean velocity profiles and (b) turbulence intensity profiles. *H*=height of the wind barrier, U_0= free-stream wind velocity (11m/s), *U(y)*= wind velocity at height *y*, *d*=distance to the barrier

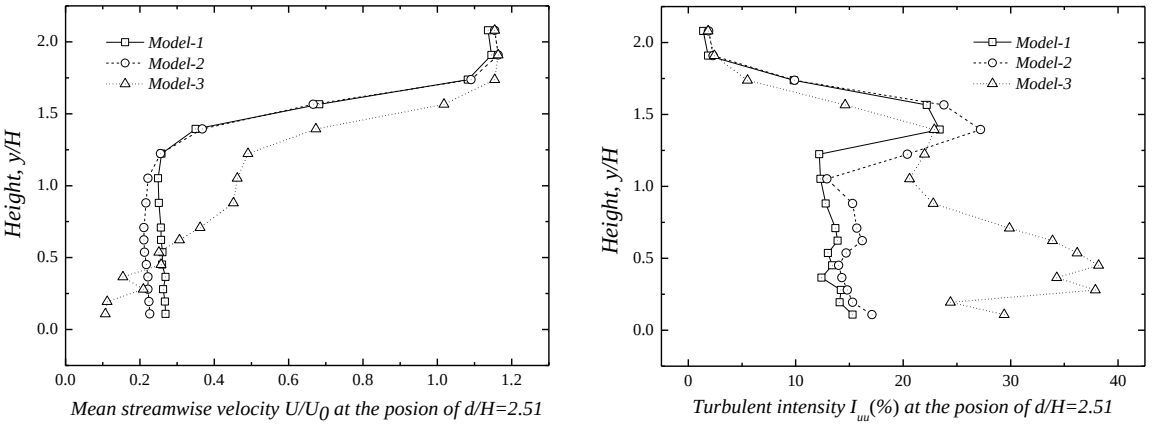

(a) (b)

Fig. 11 Mean streamwise velocity and turbulence intensity profiles of the flow field as a function of height at the position of *d/H=2.51*. (a) mean velocity profiles and (b) turbulence intensity profiles. *H*=height of the wind barrier, U_0= free-stream wind velocity (11m/s), *U(y)*= wind velocity at height *y*, *d*=distance to the barrier

3.1.2 Effects of different forms

Two different forms: porous (Model-2) and bar-type (Model-3) are used to explore the effects of different forms. Fig.7~Fig.11 show the streamwise velocity and turbulence intensity profiles of the flow field as a function of height at different positions. As shown in Fig.7 and Fig.8, the streamwise velocity and turbulence intensity profiles of the flow field are almost similar upwind of the barrier, revealing that the forms of the barrier have little impact on the characteristics of flow field upwind of the barrier. As for the flow field downwind of the barrier (Fig.9~Fig.10), the structure forms of wind barriers have a significant impact on the mean streamwise velocity and turbulence intensity profiles below the height of shear layer. Especially for the distance of 0.5H away from the barrier, great differences of mean streamwise velocity and turbulence intensity profiles under two forms of barriers are found. This is mainly because that some measured points just locate behind the barrier blades and the rest of points just are situated between the adjacent two barrier blades. So the flow fields downwind of the bar-type barrier are relatively uneven compared to the porous barrier. With the increasing of the distances away from the barrier, the difference degrees of mean streamwise velocity profiles decrease, while the differences of turbulence intensity profiles are still great. The flow field passing through porous barriers is likely to be more stable compared to the bar-type barriers. In general, the porous barrier may give a better protection than the bar-type barrier, from the aspect of flow field.

Assessment of the shelter effect of fences should consider not only the absolute reduction in wind velocity, but also the area or distance that is sheltered. So the protected distances of porous barriers and bar-type barriers are further explored. Fig.12 shows the mean streamwise velocity as a function of distance from barriers at the height of *y/H=0.54* (*y=1.88m*) above the surface of wind tunnel. The measuring height (*y=1.88m*) is close to the height of center line of the train body for CRH2 (1.95m above the orbit). Looking at the result, mean streamwise velocities downwind of the barrier are much smaller than free-stream wind velocity. With the changes of the distances away from the barrier (from -1.0H to 2.51H), the mean streamwise velocities for the height of *y/H=0.54* decrease generally. At the distance of 3.0H, the mean streamwise velocity increases obviously at the case of Model-3, while slightly increasing at the case of Model-2. With the increasing of the distance away from the barrier (from 4.0H to 8.0H), the mean streamwise velocities decrease. On the whole, the location of 8H downwind of the barrier is still in the protection zone of barriers at two cases of Model-2 and Model-3.

In order to evaluation the effect of barriers at two cases of Model-2 and Model-3. Turbulence intensity as a function of the relative distance to the wind barrier is also tested (see Fig.13). It is obviously that the turbulence intensity at the case of Model-2 is more uniform compared to the case of Model-3. With the changes of the distances away from the barrier (from -1.0H to 2.51H), the difference of turbulence intensity increases at first and then decreases.

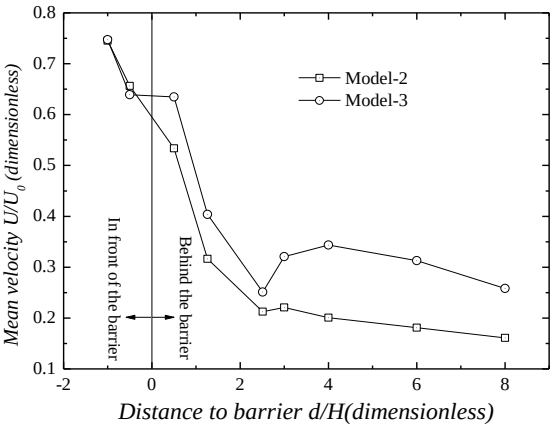

Fig. 12 Mean velocity as a function of the relative distance to the wind barrier for the height of *y/H=0.54* above the bottom of wind tunnel

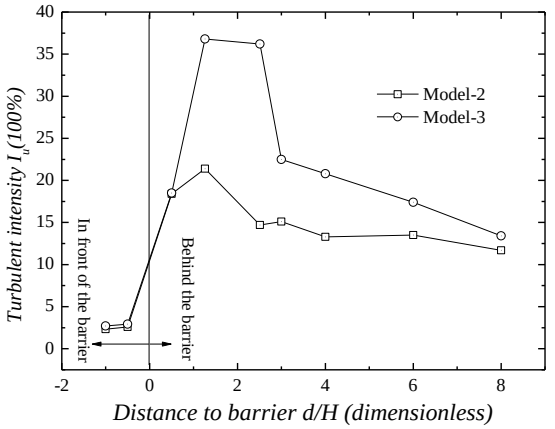

Fig. 13 Turbulence intensity as a function of the relative distance to the wind barrier for the height of *y/H=0.54* above the bottom of the wind tunnel

3.2 Aerodynamic wind loads

The aerodynamic wind loads on barrier blades have to be taken into account in design phase because they cause stress on structures which could lead to safety problems. In the force test, the form 2 is adopted. Form 2 is “long+short+long” which is composed of Blade B、Blade A and Blade C. The Blade A is used for testing (see Fig.14).

A balance (see Fig. 15) is used in the force tests whose range is 5kg and the accuracy is 0.5%. The sampling time and the sampling frequency are set as 120s and 142Hz, respectively. Besides, the sampling frequency is high enough to record the fluctuating signal of the aerodynamic forces acting on the barrier blades. The average of drag forces is used to calculate the aerodynamic coefficients.

The aerodynamics of the wind barrier blades are tested by a balance, and the drag coefficient of the barrier blade is given by

$$C_H = \frac{F_H}{0.5\rho U^2 HL} \tag{1}$$

Where, F_H is the drag force of wind barrier blades. Term H is the height of barrier blades and L is the length of barrier blades. Term U is the velocity of the approach flow and ρ is the air density.

Three kinds of wind velocities (6, 8, 10m/s) are used in the tests. The average of three corresponding results is regarded as the final value. The tested aerodynamic drag coefficients of barrier blades with respect to three cases: Model-1, Model-2 and Model-3 are depicted in Fig. 16. It can be seen that the drag coefficient (C_H) is mainly affected by the location of blades. The aerodynamic drag coefficients of barrier blades close to the wall (A1) and near the column on the right (A11) are relatively small due to the effect of wall and columns on the approach flow, possibly. From left to right (see Fig.14), drag coefficients of barrier blades at three cases increase at first and then decrease. The maximum and minimum of drag coefficients of barrier blades are 0.936 and 0.744 at the case of Model-1, respectively. The maximum and minimum of drag coefficients of barrier blades are 0.911 and 0.708 at the case of Model-2, respectively. The maximum and minimum of drag coefficients of barrier blades are 1.617 and 0.967 at the case of Model-3, respectively.

Differences of drag coefficients between Model-1 and Model-2 (The porosities of barrier blades being all 36.5%) are attributed to two aspects: fluctuating force and pore size. When free-

stream wind field passing through barriers, airflow changes to be unstable. It leads to the existing of fluctuating force, which will make a contribution to the drag force of blades and the fluctuating force is related to the pore size of the barrier blade. As for the case of Model-3, the porosities of barrier blades are 0%. So the drag coefficients of barrier blades at the case of Model-3 are larger than drag coefficients of barrier blades at the cases of Model-1 and Model-2, generally.

Firstly, the distribution law of drag coefficients of barrier blades located at different positions is investigated. Then we want to get the drag coefficients of the whole barrier. The drag coefficients of the whole barrier can be calculated by the following equations:

$$F_H = 0.5\rho U^2 C_H HL \tag{2}$$

$$\sum_{i=1} F_{Hi} = F_{HZ} \tag{3}$$

$$C_{HZ} = \frac{\sum_{i=1} C_{Hi} \times H_i}{H_Z} \tag{4}$$

Where, F_{Hi}、C_{Hi} are the drag forces and drag coefficients of wind barrier blades, respectively. F_{HZ}、C_{HZ} are the drag forces and drag coefficients of whole wind barriers, respectively. H_i (see Table 1)、H_Z (3.5m) are the heights of wind barrier blades and whole wind barriers, respectively.

The tested aerodynamic drag coefficients of whole barriers with respect to three cases: Model-1, Model-2 and Model-3 are depicted in Table2. It can be seen that the drag coefficients of porous barriers (Model-1 and Model-2) are about the same. Some differences exist between the bar-type barrier (Model-3) and porous barriers (Model-1 and Model-2). Drag coefficient of the whole barrier at case of Model-3 is the relative minimum (0.675).

Fig. 14 Distribution diagram of wind barrier blades

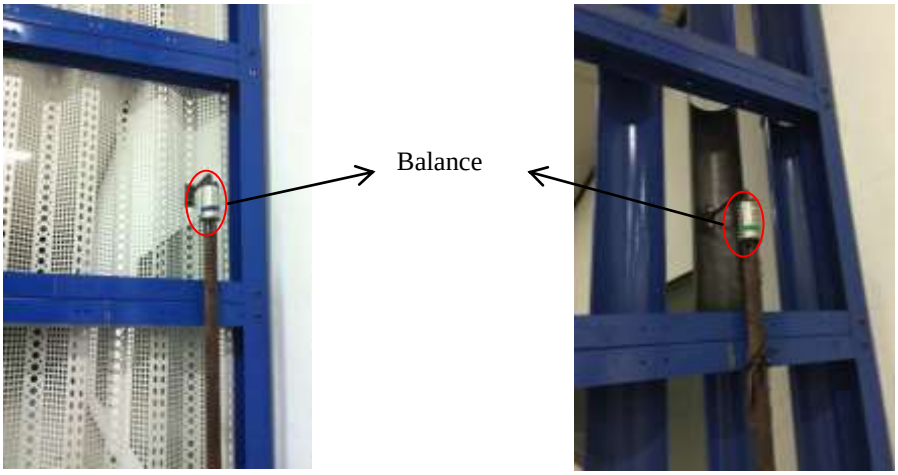

(a) Porous barrier blades (b) Bar-type barrier blades

Fig. 15 Tests of aerodynamic force for wind barriers

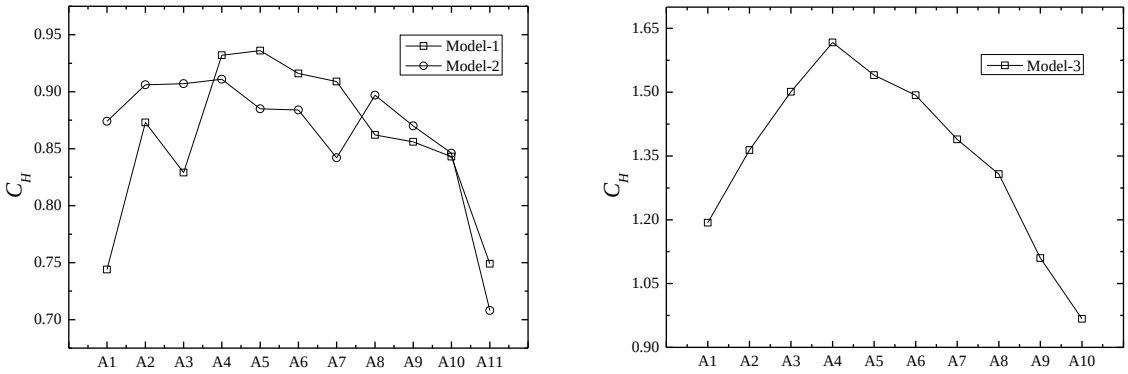

Fig. 16 Aerodynamic coefficients of barrier blades at different cases

Table2 Aerodynamic coefficients of the whole barriers at different cases

Case	Model-1	Model-2	Model-3
C_{HZ}	0.777	0.793	0.675

4. Conclusions

In the wind tunnel tests, the characteristics of flow field and aerodynamic loads of wind barrier blades were collected with respect to three cases: Model-1, Model-2 and Model-3, and then the results were analyzed and discussed. At present, the impact of scale effect has not been fully explored. So our results are more believable. The main conclusions are summarized as follows.

1) The location of barrier blades has significant impacts on the aerodynamic drag coefficients of barrier blades. Based on the experimental results, aerodynamic drag coefficients of the blades close to the wall and near the column on the right are relatively small. From left to right, drag coefficients of barrier blades at three cases increase at first and then decrease. The drag coefficients of whole barriers at three cases of Model-1, Model-2 and Model-3 are 0.777, 0.793 and 0.675, respectively.

2) Differences are great for the mean streamwise velocity profiles upwind and downwind of the barrier. There exists an obvious shear layer in the mean streamwise velocity profile downwind of the barrier. Upwind of the barrier, mean streamwise velocities increase with the

increasing of the height above the surface. At the distance of -0.5H and -1.0H away from the barrier, an intersection point is found on the profiles. Moreover, the height of intersection point is close to the height of shear layer of mean streamwise velocity profiles downwind of the barrier.

3) As for the porous barriers (Model-1 and Model-2), the pore size of the barrier blade has a slight influence on mean streamwise velocities and turbulence intensity upwind of the barrier. However, an obvious influence on mean streamwise velocities and turbulence intensity is found at the distance of 0.5H away from the barrier. At the distances of 1.26H and 2.51H, the influence on mean streamwise velocities is less obvious, while it has some influence on the turbulence intensity.

4) Slight influence of different forms of barriers (porous and bar-type) on the mean streamwise velocities and turbulence intensity is found upwind of the barrier, while great influence exists downwind of the barrier. On the whole, the mean streamwise velocities and turbulence intensity downwind of the porous barrier are more uniform than the bar-type barrier's. Moreover, values of mean streamwise velocities and turbulence intensity of the porous barrier at the same position are relatively smaller.

5) From distance of -0.5H to distance of 8H away from the barrier, mean streamwise velocities decrease generally. The turbulence intensity increases at first and then decreases. Our observations reveal that the distance of 8H downwind of the barrier is still in the effective protection area of barriers.

Acknowledgments
The research described in this paper was supported by the National Natural Science Foundation of China (Grant No. NNSF-U1334201), the National Basic Research Program of China ("973" Project) (Grant No. 2013CB036206), and the Sichuan Province Youth Science and Technology Innovation Team (Grant No. 2015TD0004).

References:

Richardsona, G. (1995), "Full-scale measurements of the effect of a porous windbreak on wind spectra", *J WIND ENG IND AEROD*., **54-55** 611-619.

Wang, D., Wang, B. and Chen, A. (2013), "Vehicle-induced aerodynamic loads on highway sound barriers part1: field experiment", *WIND STRUCT*., **17**(4), 435-449.

Dierickx, W., Gabriels, D. and Cornelis, W. (2001), "A wind tunnel study on wind speed reduction of technical textiles used as windscreen", *GEOTEXT GEOMEMBRANES*., **19**(1), 59-73.

Dierickx, W., Cornelis, W.M. and Gabriels, D. (2003), "Wind Tunnel Study on Rough and Smooth Surface Turbulent Approach Flow and on Inclined Windscreens", *BIOSYST ENG*., **86**(2), 151-166.

Dong, Z., Luo, W., Qian, G. and Wang, H. (2007), "A wind tunnel simulation of the mean velocity fields behind upright porous fences", *AGR FOREST METEOROL*., **146**(1), 82-93.

Wu, X., Zou, X., Zhang, C., Wang, R., Zhao, J. and Zhang, J. (2013), "The effect of wind barriers on airflow in a wind tunnel", *J ARID ENVIRON*., **97** 73-83.

Santiago, J.L., Martín, F., Cuerva, A., Bezdenejnykh, N. and Sanz-Andrés, A. (2007), "Experimental and numerical study of wind flow behind windbreaks", *ATMOS ENVIRON*., **41**(30), 6406-6420.

Bitog, J.P., Lee, I.B., Shin, M.H., Hong, S.W., Hwang, H.S., Seo, I.H., Yoo, J.I., Kwon, K.S., Kim, Y.H. and Han, J.W. (2009), "Numerical simulation of an array of fences in Saemangeum reclaimed land", *ATMOS ENVIRON*., **43**(30), 4612-4621.

Telenta, M., Batista, M., Biancolini, M.E., Prebil, I. and Duhovnik, J. (2015), "Parametric numerical study of wind barrier shelter", *WIND STRUCT*., **20**(1), 75-93.

Huoyue, X., Yongle, L. and Bin, W. (2015), "Aerodynamic interaction between static vehicles and wind barriers on railway bridges exposed to crosswinds", *WIND STRUCT*., **20**(2), 237-247.

Suzuki, M., Tanemoto, K. and Maeda, T. (2003), "Aerodynamic characteristics of train/vehicles under cross winds", *J WIND ENG IND AEROD*., **91**(1–2), 209-218.